International Journal of Electrical and Computer Engineering (IJECE)
Vol. 9, No. 4, August 2019, pp. 2513~2522
ISSN: 2088-8708, DOI: 10.11591/ijece.v9i4.pp2513-2522

The neural network-combined optimal control system of induction motor

Trong-Thang Nguyen
Faculty of Energy Engineering, Thuyloi University, Vietnam

Article Info

Article history:

Received Feb 13, 2019
Revised Feb 23, 2019
Accepted Mar 12, 2019

Keywords:

Induction motor
LQR control
Neural network
Optimal control

ABSTRACT

This research aims to propose the optimal control method combined with the neuron network for an induction motor. In the proposed system, the induction motor is a nonlinear object which is controlled at each working point. At these working-points, the state equation of the induction motor is linear, so it is possible to apply the linear quadratic regular algorithm for the induction motor. Therefore, the parameters of the state feedback controller are the functions. The output-input relationships of these functions are set through the neural network. The numerical simulation results show that the quality of the control system of the induction motor is very high: The response speed always follows the desired speed with the short transition time and the small overshoot. Furthermore, the system is robust in the case of changing the load torque, and the parameters of the induction motor are incorrectly defined.

Copyright © 2019 Institute of Advanced Engineering and Science.
All rights reserved.

Corresponding Author:

Trong-Thang Nguyen,
Faculty of Energy Engineering,
Thuyloi University,
175 Tay Son, Dong Da, Hanoi, Vietnam.
Email: nguyentrongthang@tlu.edu.vn

1. INTRODUCTION

The induction motor is applied widely in practical industrial [1] because of the low weight per power- unit, high robustness, high reliability, and low cost [2]. There are many methods for controlling the induction motor with the high performance, such as the scalar control [3], the indirect field orientation control [4], the direct torque control [5], and the field orientation control [6, 7].

It is difficult to control the induction motor because of its nonlinearities, so some nonlinear methods have been applied to control the induction motor. For example, the control method is based on a flatness principle [8, 9], but the disadvantage of this method is the need of knowing exactly the parameters of the induction motor. Another method is an accurate linearization method [10, 11], the purpose of this method is to convert the input-output relationship of induction motor into a linear one by separating the nonlinear components in the inner loop. The disadvantage of this method is that if the nonlinear components are removed incorrectly, it will adversely affect the control results and reduce the sustainability of the system. Other nonlinear control methods such as bakstepping [12-14], sliding mode control [15-16], the disadvantage of these methods is that there are harmonic oscillations.

A method promises high-quality control and efficiency that is the control method based on Linear Quadratic Regular (LQR) algorithm. The LQR method is used to control a lot of objects in practice as wind power generator [17], converter [18], quad-rotor [19], two-wheels self-balancing mobile robot [20]. The LQR method is built by using a mathematical algorithm to minimize the cost function with weighting factors defined by the designer. The cost-function is often defined as a sum of the deviations of response output and their desired values [21].

To apply the LQR method for the induction motor, the controller is designed for the induction motor at the different working-points. At each different working point, the state feedback matrix of the controller is

different, so each component in the state feedback matrix is a function. To establish the output-input relationship of these functions, an artificial neural network is used. The result is an optimal control system for the nonlinear induction motor with the high-quality.

2. THE LINEAR QUADRATIC REGULAR ALGORITHM

Considering the state equation of the object:

$$\dot{x}(t) = A.x(t) + B.u(t) \tag{1}$$

where:

$x(t) = [x_1(t), x_2(t),..., x_n(t)]$ is the state signal vector,

$u(t) = [u_1(t), u_2(t),..., u_m(t)]$ is the control signal vector.

The requirement of the control system is finding the control signal $u(t)$ in order for the control-object is operated from the initial-state $x(t_0) = x(0)$ go to the end-state $x(t_f) = 0$ and satisfy the following condition (cost function):

$$J = \frac{1}{2}x^T(t_f).M.x(t_f) + \frac{1}{2}\int_{t_0}^{t_f}[x^T(t).Q.x(t) + u^T(t).R.u(t)]dt \to \min \tag{2}$$

where *Q* and M are the symmetric, positive semi-definite weight matrix. *R* is the symmetric, positive definite weight matrix. To solve the problem, we establish the Hamilton function:

$$H = \frac{1}{2}[x^T(t).Q.x(t) + u^T(t).R.u(t)] + \lambda^T[A.x(t) + B.u(t)] \tag{3}$$

The optimal control-signal must satisfy the following equations:

- The state equation:

$$\dot{x}(t) = A.x(t) + B.u(t) \tag{4}$$

- The equilibrium equation:

$$\dot{\lambda}(t) = -\frac{\partial H}{\partial x} = -Q.x(t) - A.\lambda^T(t) \tag{5}$$

- The optimal condition:

$$\frac{\partial H}{\partial u} = R.u(t) + B^T.\lambda^T(t) = 0 \tag{6}$$

From equation (6), we have:

$$u(t) = -R^{-1}.B^T.\lambda^T(t) \tag{7}$$

Replace $u(t)$ into (4), we have:

$$\dot{x}(t) = A.x(t) - B.R^{-1}.B^T.\lambda^T(t) \tag{8}$$

Combining (8) and (5) we have:

$$\begin{bmatrix} \dot{x}(t) \\ \dot{\lambda}(t) \end{bmatrix} = \begin{bmatrix} A & -B.R^{-1}.B^T \\ -Q & -A \end{bmatrix} \begin{bmatrix} x(t) \\ \lambda^T(t) \end{bmatrix} \tag{9}$$

Solving the above equations, we have the optimal control signal:

$$u^*(t) = -K(t).x(t) \tag{10}$$

where $K(t) = R^{-1}.B^T.P(t)$

$P(t)$ is the positive semi-definite solution of the Riccati equation:

$$-\dot{P} = P.A + A^T.P + Q - P.B.R^{-1}.B^T.P \tag{11}$$

In the case of the infinite time $t_f = \infty$, the cost function is as follows:

$$J = \frac{1}{2}\int_0^{t_f} [x^T(t).Q.x(t) + u^T(t).R.u(t)]dt \rightarrow \min \tag{12}$$

The optimal control signal:

$$u^*(t) = -K.x(t) \tag{13}$$

where $K = R^{-1}.B^T.P$

P is the positive semi-definite solution of the Riccati equation:

$$P.A + A^T.P + Q - P.B.R^{-1}.B^T.P = 0 \tag{14}$$

3. THE SYSTEM MODEL OF THE INDUCTION MOTOR DRIVE

The induction motor drive is controlled based on the axis oriented along the stator-flux *dq*. The control diagram is shown in Figure 1.

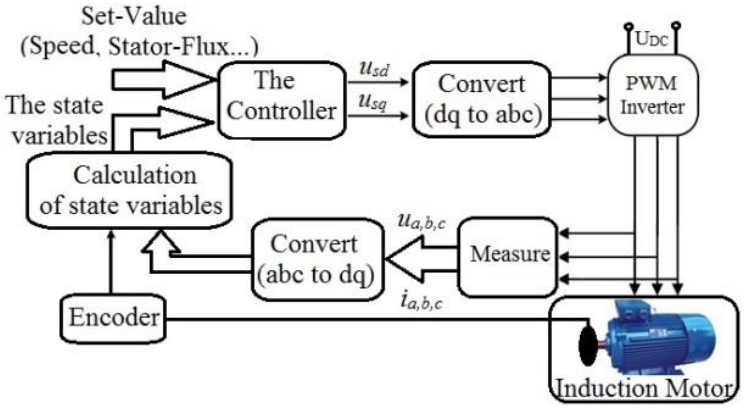

Figure 1. The control diagram of the induction motor drive

Considering the equations of cage induction motor on the *dq*-axis oriented along the stator-flux that rotes with the speed ω_ψ , the voltage vector of the stator and rotor are presented [1]:

$$\underline{u}_s = R_s.\underline{i}_s + \frac{d(\underline{\psi}_s)}{dt} + j.\omega_\psi.\underline{\psi}_s \quad (15)$$

$$\underline{u}_r = R_r.\underline{i}_r + \frac{d(\underline{\psi}_r)}{dt} + j.(\omega_\psi - p.\omega).\underline{\psi}_r \quad (16)$$

where $\underline{u}_s, \underline{u}_r$ are the vectors of stator and rotor voltage on *dq* axis; $\underline{i}_s, \underline{i}_r$ are the vectors of stator and rotor current on *dq* axis; $\underline{\psi}_s, \underline{\psi}_r$ are the vectors of stator and rotor flux on *dq* axis; R_s is the stator resistance, R_r is the rotor resistance; ω_ψ is the angular speed of stator-flux.

The flux vector of stator and rotor:

$$\underline{\psi}_s = \underline{i}_s.L_s + \underline{i}_r.L_m \quad (17)$$

$$\underline{\psi}_r = \underline{i}_r.L_r + \underline{i}_s.L_m \quad (18)$$

where L_s is the stator inductances, L_r is the rotor inductances, L_m is the mutual inductance

The motion equation:

$$J\frac{d\omega}{dt} = T_E - T_L \quad (19)$$

$$T_E = \frac{3}{2}p.(\underline{\psi}_s.\underline{i}_s) \quad (20)$$

where ω is the angular speed of the rotor, T_E the electromagnetic torque, T_L is the load torque, *p* is the number of pole pairs. Because we're considering on the axis oriented along the stator-flux that rotes with the speed of ω_ψ , so $\psi_{sd} = \underline{\psi}_s$, $\psi_{sq} = 0$. Rewriting the equations (15-20) according to *d*-axis and *q*-axis components, we have:

$$u_{sd} = R_s.i_{sd} + \frac{d(\psi_{sd})}{dt} \quad (21)$$

$$u_{sq} = R_s.i_{sq} + \omega_\psi.\psi_{sd} \quad (22)$$

$$u_{rd} = R_r.i_{rd} + \frac{d(\psi_{rd})}{dt} - (\omega_\psi - p.\omega).\psi_{rq} = 0 \quad (23)$$

$$u_{rq} = R_r.i_{rq} + \frac{d(\psi_{rq})}{dt} + (\omega_\psi - p.\omega).\psi_{rd} = 0 \quad (24)$$

$$\psi_{sd} = i_{sd}.L_s + i_{rd}.L_m \quad (25)$$

$$\psi_{sq} = i_{sq}.L_s + i_{rq}.L_m \quad (26)$$

$$\psi_{rd} = i_{rd}.L_r + i_{sd}.L_m \quad (27)$$

$$\psi_{rq} = i_{rq}.L_r + i_{sq}.L_m \quad (28)$$

$$J\frac{d\omega}{dt} = \frac{3}{2}p.(\psi_{sd}.i_{sq}) - T_L \quad (29)$$

where u_{sd}, u_{sq} are the stator voltage component of *d*-axis and *q*-axis; u_{rd}, u_{rq} are the rotor voltage component of *d*-axis and *q*-axis; i_{sd}, i_{sq} are the stator current component of *d*-axis and *q*-axis; i_{rd}, i_{rq} are the rotor current component of *d*-axis and *q*-axis; ψ_{sd}, ψ_{sq} are the stator-flux component of *d*-axis and *q*-axis; ψ_{rd}, ψ_{rq} are the rotor-flux component of *d*-axis and *q*-axis.

Eliminating the variables $i_{rd}, i_{rq}, \psi_{rd}, \psi_{rq}$ in equations (21-29), we obtain the following equations:

$$\begin{cases} \dfrac{di_{sd}}{dt} = -\dfrac{L_s.R_r + L_r.R_s}{L_s.L_r - L_m^2}.i_{sd} + (\omega_\psi - p.\omega).i_{sq} + \dfrac{R_r}{L_s.L_r - L_m^2}.\psi_{sd} + \dfrac{L_r}{L_s.L_r - L_m^2}.u_{sd} \\ \dfrac{di_{sq}}{dt} = -(\omega_\psi - p.\omega).i_{sd} - \dfrac{L_s.R_r}{L_s.L_r - L_m^2}.i_{sq} + \dfrac{(\omega_\psi - p.\omega).L_r}{L_s.L_r - L_m^2}.\psi_{sd} \\ \dfrac{d\psi_{sd}}{dt} = -R_s.i_{sd} + u_{sd} \\ \dfrac{d\omega}{dt} = -\omega_\psi.\dfrac{3.p.\psi_{sd}}{2.J.R_s}\psi_{sd} + \dfrac{3.p.\psi_{sd}}{2.J.R_s}u_{sq} \end{cases} \quad (30)$$

Equation (30) is the state equation. Where $\underline{x} = [x_1, x_2, x_3, x_4]^T = [i_{sd}, i_{sq}, \psi_{sd}, \omega]^T$ is the state signal vector. $\underline{u} = [u_1, u_2]^T = [u_{sd}, u_{sq}]^T$ is the control signal vector.

4. DESIGNING THE NEURON NETWORK COMBINED-OPTIMAL CONTROLLER

Designing the controller for cage induction motor with the parameters shown in Table 1.

Table 1. The parameters of induction motor

Rs(Ω)	Ls(H)	Rr(Ω)	Lr(H)	Lm(H)	J(kg.m^2)	*p*
1.55	0.098	1.31	0.097	0.0917	0.14	3

We design the control signal $\underline{u}(t) = -K.\underline{x}(t)$ in order for $\lim_{t\to\infty}(\underline{x}_{response} - \underline{x}_{set}) \to 0$.

Named $\underline{x}_e$ is the error between $\underline{x}_{response}$ and $\underline{x}_{set}$.

$\underline{x}_e = (\Delta x_1 = x_{1\_response} - x_{1\_set}, \Delta x_2 = x_{2\_response} - x_{2\_set}, \Delta x_3 = x_{3\_response} - x_{3\_set}, \Delta x_4 = x_{4\_response} x - x_{4\_set})$

The state equation (30) is rewritten as follows:

$$\dot{\underline{x}}_e = A.\underline{x}_e + B.\underline{u}_e \quad (31)$$

where $\underline{u}_e = \underline{u} - \underline{u}_{set}$.

$\underline{u}$ and $\underline{u}_{set}$ are control signals in order for the status signals reach the $\underline{x}_{response}$ and $\underline{x}_{set}$ values respectively.

The matrices of state equations are as follows:

$$A=\begin{bmatrix} -\frac{L_s.R_r+L_r.R_s}{L_s.L_r-L_m^2} & \omega_\psi - p.\omega & \omega_\psi - p.\omega & 0 \\ -(\omega_\psi - p.\omega) & -\frac{L_s.R_r}{L_s.L_r-L_m^2} & \frac{(\omega_\psi - p.\omega).L_r}{L_s.L_r-L_m^2} & 0 \\ -R_s & 0 & 0 & 0 \\ 0 & 0 & -\omega_\psi.\frac{3.p.\psi_{sd}}{2.J.R_s} & 0 \end{bmatrix} \quad (32)$$

$$B=\begin{bmatrix} \frac{L_r}{L_s.L_r-L_m^2} & 0 \\ 0 & 0 \\ 1 & 0 \\ 0 & \frac{3.p.\psi_{sd}}{2.J.R_s} \end{bmatrix} \quad (33)$$

Suppose we always control the system to satisfy the condition $\psi_{sd}=\psi_{set}=const$, so the matrix $B=const$. The matrix A is changed because of the change of two components $(\omega_\psi - p.\omega)$ and ω_ψ. Therefore, in the case of each pair of values $(\omega_\psi - p.\omega)$ and ω_ψ, we will find the optimal control signals respectively.

The main missions of the control system are that $\psi_{sd}->\psi_{set}, \omega->\omega_{set}$, so the output of system is as follows:

$$\underline{y}=\underline{r}=C.\underline{x}_{set} \quad (34)$$

$$C=[0\ \ 0\ 1\ \ 1]^T \quad (35)$$

Considering the state equation (31), at the equilibrium, we have:

$$\underline{x}_{set}=A^{-1}.B.\underline{u}_{set} \quad (36)$$

Combining equation (34) and equation (36), we have:

$$\underline{u}_{set}=-[C.A^{-1}.B]^{-1}\underline{r} \quad (37)$$

The optimal control signal for the system (31) is as follows:

$$\underline{u}_e=-K.\underline{x}_e \quad (38)$$

where:

$$K=R^{-1}.B^T.P \quad (39)$$

P is the positive semi-definite solution of the Riccati equation:

$$P.A + A^T.P + Q - PBR^{-1}.B^T.P = 0 \quad (40)$$

According to equation (38), we have:

$$\begin{aligned} \underline{u} &= \underline{u}_{set} - K.(\underline{x}_{response} - \underline{x}_{set}) \\ &= -K.\underline{x}_{response} + \underline{u}_{set} - K.\underline{x}_{set} \\ &= -K.\underline{x}_{response} - [C.A^{-1}.B]^{-1}\underline{r} + K.A^{-1}.B.[C.A^{-1}.B]^{-1}\underline{r} \\ &= -K.\underline{x}_{response} - K_r\underline{r} \end{aligned} \quad (41)$$

where:

$$K_r = [K_{LQR}.A^{-1}.B - I].[C.A^{-1}.B]^{-1} \quad (42)$$

Therefore, the control diagram is shown as Figure 2.

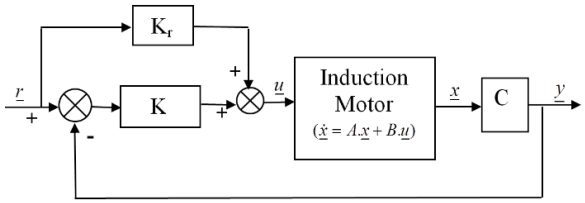

Figure 2. The control diagram

In the above control diagram, the matrices (*A, B, C)* are known, we must find the matrix K according to the formula (39), then find the matrix K_r according to the formula (42). Because of the control purposes are that $\psi_{sd} -> \psi_{set}, \omega -> \omega_{set}$, we install the *Q*, *R* matrices that meet the requirements are as follows:

$$Q = diag(10^{-3}, 10^{-3}, 2.10^{-2}, 10^{-2}) \quad (43)$$

$$R = diag(2.10^{-7}, 2.10^{-7}) \quad (44)$$

The matrix *A* is changed due to the variation of two components $(\omega_\psi - p.\omega)$ and ω_ψ. Therefore, in the case of each pair $(\omega_\psi - p.\omega)$ and ω_ψ, we will find each feedback matrix K with the size is *2x4*. We set up an off-line trained neuron network to describe the relationship between the matrix K and $[(\omega_\psi - p.\omega), \omega_\psi]$. A neural network includes many simple components, these components are the single-input neuron or the multiple-input neuron, are shown as the Figure 3 [22].

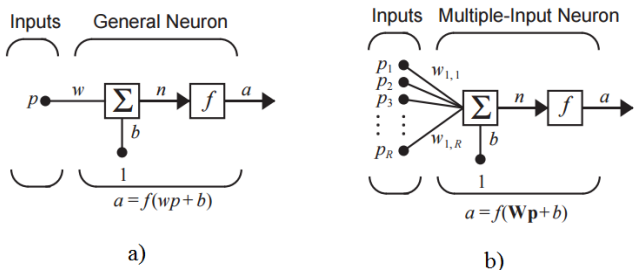

Figure 3. The component of neural network: a) the case of single-input, b) the case of multiple-input

Usually, a neural network has several layers. For example, Figure 4 shows the neural network with three layers, the outputs of the first layer is the input of the second layer, the outputs of second layer is the input of the third layer. The output layer is at once with whose output is the network output, the other layers are named hidden layer.

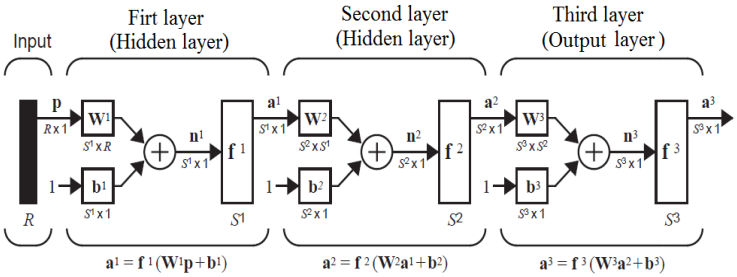

Figure 4. The neural network with three layers

To meet the requirements of the control system, we set up the neuron network as follows: The feed-forward neural network includes three layers: the first layer is the input which includes two signals $(\omega_\psi - p.\omega)$ and ω_ψ ; The second layer is hidden; the last layer is the output, it includes 8 signals which are the components of the matrix *K(*2x4*)*. The transfer-function of the first layer and second layer are *tansig*. The transfer-function of the last layer is *pureli*.

The diagram of neural network training is shown in Figure 5. The training results are characteristics of the relationship between the matrix *K* and $[(\omega_\psi - p.\omega), \omega_\psi]$, which are shown in Figure 6.

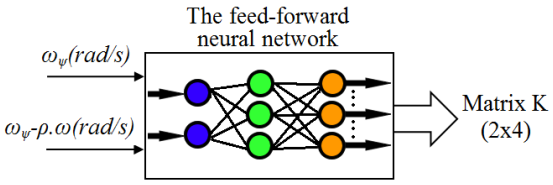

Figure 5. The diagram of neural network training

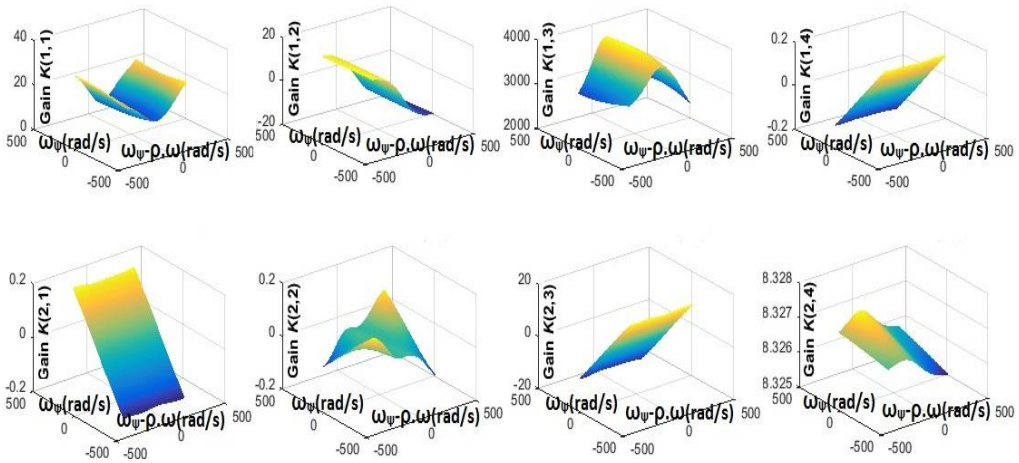

Figure 6. The characteristics of the relationship between the matrix *K* and $[(\omega_\psi - p.\omega), \omega_\psi]$

5. RESULTS AND ANALYSIS

Running the system with the parameters of the induction motor listed in Table 1 and the controller parameters are set up in section 4. The simulation results are shown in Figure 7(a), it includes the following characteristic: the desired speed, the response speed and the load torque. The results show that the response speed always follows the set speed with very short transition time, there is not overshot. Furthermore, when changing the disturbance (load torque TL), the response speed is almost unaffected by the change of the load torque. To more clearly, the zoom-in simulation results are shown in Figure 7(b).

The results of controlling the stator-flux are shown in Figure 8. The results show that the response flux always follows the set flux with the static error of zero. To investigate the sustainability of the proposed control method, the author runs the control system in the case of the difference between the actual parameter and the parameter used for the controller. The details are as follows: Rr.70%; Lr.130%; Rs.130%; J.130%. The results are shown in Figure 9. The results show that the quality of the system is almost unaffected when there are inaccuracies of induction motor parameters. Therefore, we can conclude that the proposed control system has a high quality and high sustainability.

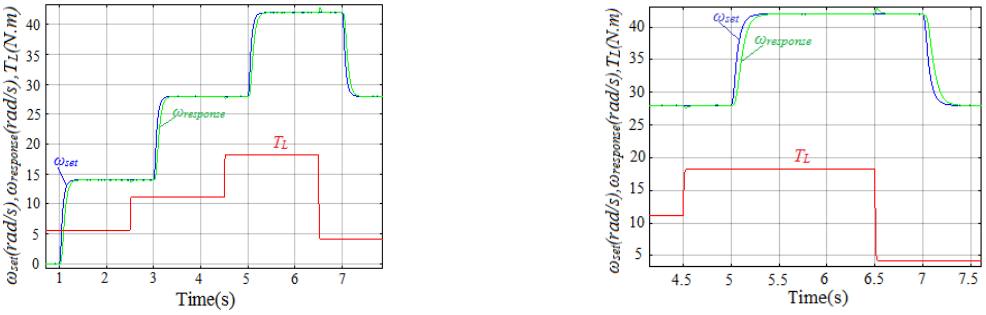

Figure 7. The simulation results in the case of the accurate parameters:
a) the normal view, b) the zoom-in view

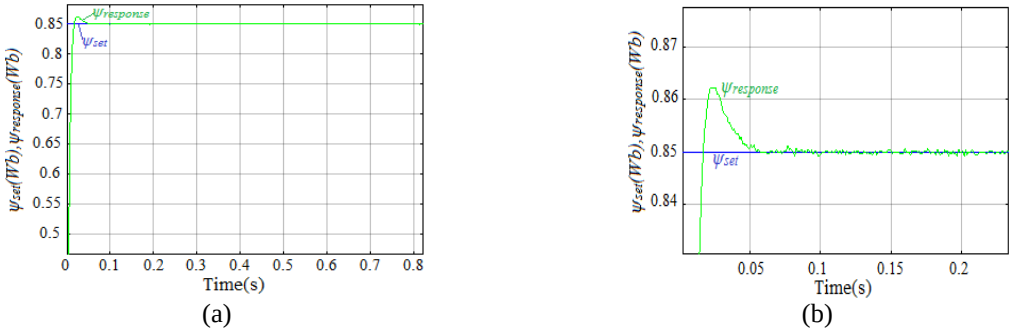

Figure 8. The results of controlling the stator-flux: a) the normal view, b) the zoom-in view

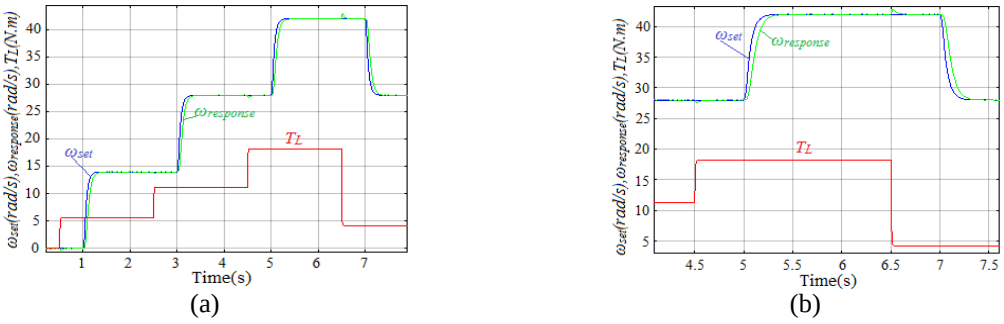

Figure 9. The simulation results in the case of the inaccuracies parameters:
a) the normal view, b) the zoom-in view

6. CONCLUSION

In this study, the author has succeeded in building the optimal controller combined with the neuron network for the induction motor. The results show that the control quality of the system is very high: The response speed always follows the desired speed with the short transition time and the small overshoot. Moreover, the control system is very stable in the case of changing the load torque, and in the case of inaccuracies of induction motor parameters. The success of the proposed method is base for applying the control algorithm to electric motion using the induction motor in the industries.

REFERENCES

[1] A. Ramesh, *et al.*, "A Novel Three Phase Multilevel Inverter with Single Dc Link for Induction Motor Drive Applications," *International Journal of Electrical and Computer Engineering (IJECE)*, vol/issue: 8(2), pp. 763-770, 2018.

[2] I. Takahashi and Y. Ohmori, "High-performance direct torque control of an induction motor," *IEEE Transactions on Industry Applications*, vol/issue: 25(2), pp. 257-264, 1989.

[3] D. Karthik and T. R. Chelliah, "Analysis of scalar and vector control based efficiency-optimized induction motors subjected to inverter and sensor faults," *Advanced Communication Control and Computing Technologies (ICACCCT), 2016 International Conference on*, pp. 462-466, 2016.

[4] L. Liu, *et al.*, "Indirect field-oriented torque control of induction motor considering magnetic saturation effect: error analysis," *IET Electric Power Applications*, vol/issue: 11(6), pp. 1105-1113, 2017.

[5] M. P. Kazmierkowski and A. B. Kasprowicz, "Improved direct torque and flux vector control of PWM inverter-fed induction motor drives," *IEEE Transactions on industrial electronics*, vol/issue: 42(4), pp. 344-350, 1995.

[6] M. E. Saadi, *et al.*, "Using the Five-Level NPC Inverter to Improve the FOC Control of the Asynchronous Machine," *International Journal of Power Electronics and Drive Systems (IJPEDS)*, vol/issue: 9(8), pp. 1457-1466, 2018.

[7] H. Tajima and Y. Hori, "Speed sensorless field-orientation control of the induction machine," *IEEE transactions on industry applications*, vol/issue: 29(1), pp. 175-180, 1993.

[8] L. Fan and L. Zhang, "Fuzzy based flatness control of an induction motor," *Procedia Engineering*, vol. 23, pp. 72-76, 2011.

[9] J. Dannehl and F. W. Fuchs, "Flatness-based control of an induction machine fed via voltage source inverter-concept, control design and performance analysis," *IEEE Industrial Electronics, IECON 2006-32nd Annual Conference on*. IEEE, pp. 5125-5130, 2006.

[10] M. Bodson, *et al.*, "High-performance induction motor control via input-output linearization," *IEEE control systems*, vol/issue: 14(4), pp. 25-33, 1994.

[11] C. P. Zhang, *et al*., "Nonlinear control of induction motors based on direct feedback linearization," *Proceedings of the CSEE*, vol. 2, pp. 021, 2003.

[12] A. Abdallah, *et al.*, "Double star induction machine using nonlinear integral backstepping control," *International Journal of Power Electronics and Drive Systems (IJPEDS)*, vol/issue: 10(1), pp. 27-40, 2019.

[13] S. Drid, *et al.*, "Robust backstepping vector control for the doubly fed induction motor," *IET Control Theory & Applications*, vol/issue: 1(4), pp. 861-868, 2007.

[14] J. Zhou and Y. Wang, "Real-time nonlinear adaptive backstepping speed control for a PM synchronous motor," *Control Engineering Practice*, vol/issue: 13(10), pp. 1259-1269, 2005.

[15] Z. Yan, *et al.*, "Sensorless sliding-mode control of induction motors," *IEEE Transactions on Industrial Electronics*, vol/issue: 47(6), pp. 1286-1297, 2000.

[16] M. Habbab, *et al.*, "Real Time Implementation of Fuzzy Adaptive PI-sliding Mode Controller for Induction Machine Control," *International Journal of Electrical and Computer Engineering (IJECE)*, vol/issue: 8(5), pp. 2884, 2018.

[17] T. P. T. Slavov, "LQR power control of wind generator," *2018 Cybernetics & Informatics (K&I)*, IEEE, pp. 1-6, 2018.

[18] E. Rakhshani, *et al.*, "PSO-based LQR controller for multi modular converters," *ECCE Asia Downunder (ECCE Asia), 2013 IEEE*, pp. 1023-1027, 2013.

[19] C. Liu, *et al.*, "PID and LQR trajectory tracking control for an unmanned quadrotor helicopter: Experimental studies," *Control Conference (CCC), 2016 35th Chinese*, IEEE, pp. 10845-10850, 2016.

[20] J. Zhao and X. Ruan, "The LQR control and design of dual-wheel upright self-balance Robot," *Intelligent Control and Automation*, pp. 4864-4869, 2008.

[21] Lewis, *et al.*, "Optimal control," John Wiley & Sons, 2012.

[22] T. T. Nguyen, "The neural network-based control system of direct current motor driver," *International Journal of Electrical and Computer Engineering (IJECE)*, vol/issue: 9(2), pp. 1145-1452, 2019.